

CW Argon-ion Laser Crystallization of a-Si:H Thin Films

A. Sunda-Meya*, D. Gracin*†, J. Dutta*, B. Vlahovic*, R.J. Nemanich**,

*Department of Physics, North Carolina Central University, Durham, NC

**Department of Physics, North Carolina State University, Raleigh, NC

†On leave from Materials Science Division, Rudjer Boskovic Institute, Zagreb, Croatia

ABSTRACT

Thin a-Si:H films, with a thickness of 1 μm , with different hydrogen concentrations, prepared by hot wire deposition were crystallized by 514.5 nm cw Ar ion laser radiation, with a power density between 150 and 270 kW/cm^2 . The crystallization was continuously monitored by Raman spectroscopy for exposures up to hours. The analysis of crystallization process using Johnson-Mehl phenomenological equations showed an apparent crystallization energy of around 0.5 eV and low dimensional crystal growth. The mean value of the crystal size decreases with increasing irradiation energy and initial hydrogen content and varies between 3 and 6 nm.

INTRODUCTION

The crystallization process of amorphous silicon films on glass substrates is important from a technological point of view for its potential use in the production of hybrid, amorphous/poly-crystalline silicon solar cells (1-5). Laser crystallization appears to be more promising compared to thermal crystallization because it overcomes the conflicting requirements of high temperature for crystallization and low temperature for not destroying the glass substrate, by depositing almost all of the laser energy directly into the silicon film (6).

From the scientific point of view, while there has been extensive work in the field, there remains significant details that are not well understood (7).

EXPERIMENTAL

The 1 μm thick amorphous silicon films, prepared by hot wire deposition plasma enhanced chemical vapour deposition (HW PECVD) on a glass and monocrystalline silicon substrate, were illuminated with 514.5 nm radiation from an Ar ion laser. The laser beam was focused through the optical system on a spot with diameter of about 5 μm . The laser irradiation power density was varied between 150 and 270 kW/cm^2 and irradiation times were between 0.85 h and 2 h. During the laser exposure, the Raman spectra were measured by using an Innova Ar ion laser and a U1000 ISA spectrometer, equipped with an Olympus microscope and photomultiplier detector.

The hydrogen concentration was estimated from FTIR spectroscopic data using the method described in ref (10). The average temperature in the irradiated volume was estimated from the ratio of Stokes and anti-Stokes intensities using the procedure described in ref (8), (9). This approach typically yields absolute values, which are too low by about 100K, but the relative temperatures are more accurate.

RESULTS AND DISCUSSION

At the beginning of the annealing procedure, the Raman spectra are typical of amorphous silicon, with a pronounced, broad TO peak at about 480 cm^{-1} and a broad TA peak at 150 cm^{-1} . Shortly after initiating the laser exposure, the peaks corresponding to amorphous phase became very weak and disappeared while the TO peak, corresponding to crystalline silicon, between 490 and 510 cm^{-1} , begins to grow. During the irradiation, the peak area, A , peak position, ω_{TO} , and peak width, FWHM (full width at half maximum), change, depending on the illumination power density. However, these changes have qualitatively the same behavior and can be divided in two regimes. Spectra for a typical example, obtained at an illumination power density of 230 kW/cm^2 , are displayed in Fig 1. At the initiation of illumination (Fig.1.a), the peak area increase while the TO peak position shifts first towards lower wave numbers and later in the opposite direction. During the first regime, the area under the TO peak reaches its saturation value. In the next regime (Fig.1b), only the position of peak maximum and the FWHM change. Eventually, the process reaches saturation values.

The changes are presented more quantitatively in the next figures. As is shown in Fig. 2, the saturation values of the area under the TO peak, A_{sat} , differ by an order of magnitude when the energy density is changed from 150 to 230 kW/cm^2 . However, the time dependence of the ratio of the peak area to the saturation value, $A(t)/A_{\text{sat}}$, show a similar type of behaviour (see Fig. 3).

The data can be analysed by using the Johnson-Mehl equations (11), which can be expressed as

$$X(t) = 1 - \exp(-(Kt)^n) \quad (1)$$

where $X(t)$ is the area ratio, $A(t)/A_{\text{sat}}$, t is the irradiation time, K is a rate constant, and n is the growth exponent. If the crystallization process is mainly thermally activated, then K is given by

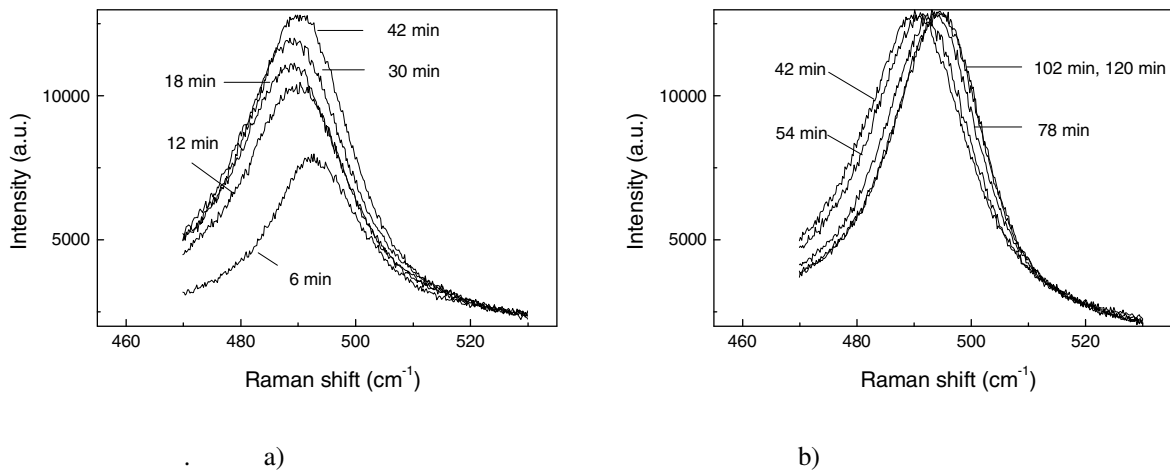


Fig.1. Raman spectra measured during the illumination with power density of 230 kW/cm^2 , for illumination time $t \leq 42 \text{ min}$ (a) and $t \geq 42 \text{ min}$ (b).The illumination time is denoted on each spectrum.

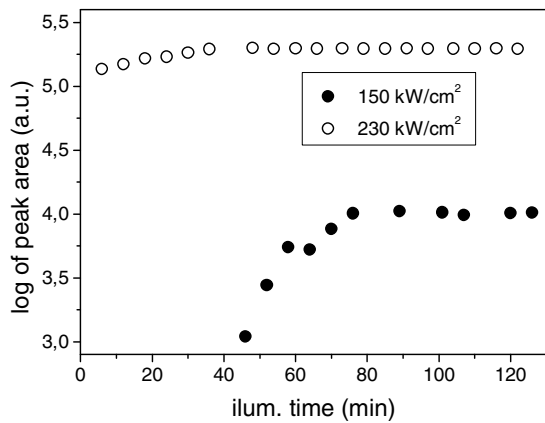


Fig. 2. The logarithm of area under TO peak versus irradiation time for two extreme values of irradiation power (shown in the graph).

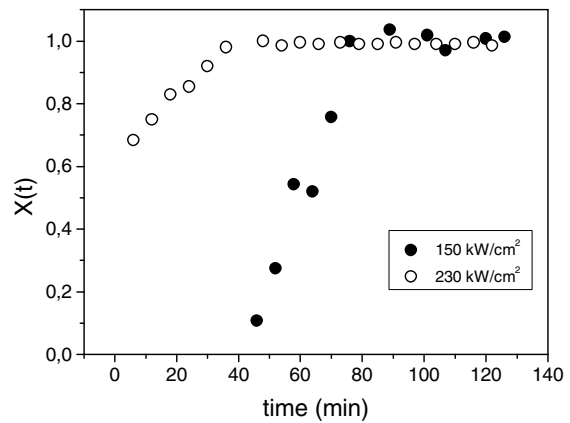


Fig. 3. The ratio of area under TO peak after illumination time, $A(t)$ and saturation area A_{sat} , $X(t)=A(t)/A_{sat}$, versus illumination time, t , for two irradiation powers.

the relation

$$K=K_o \exp(-(\Delta E/kT)) \quad (2)$$

where K_o is a constant, ΔE is the overall activation energy, k is the Boltzman constant and T is the temperature in Kelvin.

Analyzing the results according to the above relations, we obtain a value of $\Delta E \approx 0.5$ eV and values for n between 1 and 2 which suggest a low dimensionality of crystal growth.

The frequency of the TO peak, after the instability at the start of the process, shifts towards higher values during illumination (Fig. 4). Its initial and final values are substantially lower for higher illumination power. In Fig. 4 the values for peak positions are corrected to zero temperature in order to compare Raman measurements performed under different illumination power, e.g. different temperature. This was done by correcting the data based on the temperature dependent shifts of single crystal silicon determined according to Hart et al.(12).

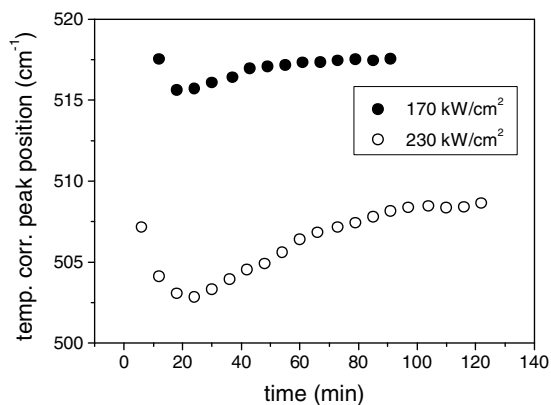


Fig. 4. The frequency of TO phonon peak as a function of illumination time for two extreme power densities.

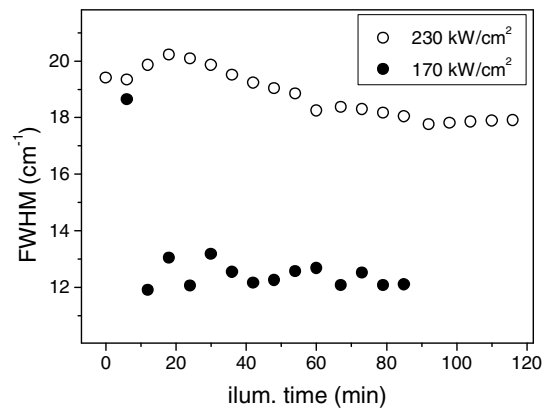


Fig. 5. The full width at half maximum of TO phonon peak versus illumination time for two extremes of power densities.

The TO peak position of polycrystalline silicon is a function of crystal size, temperature (13) and strain in the material (14). Since in our case, the temperature rise due to laser irradiation is low, the crystallization is only partial, and there is a high probability that the crystal grains are embedded in the amorphous phase, which should lower the strain in material. For this reason we will only consider the influence of crystal size and temperature.

In general, as the temperature of the sample is increased the peak frequency becomes lower. Similarly, as the crystal size is decreased below 100 nm, the peak frequency becomes lower. If the temperature of the sample is constant, then the peak position can be used as an estimation of the crystal size. Unfortunately, the temperature is not constant during the process studied here. The temperature rise, ΔT , due to laser light absorption can be expressed by the relation (15)

$$\Delta T = (1-R) N/\kappa (P/w) \quad (3)$$

where R is the reflectivity of the sample, P is the laser power, κ is thermal conductivity, and N is a slowly varying function of the product of absorption coefficient α and laser beam diameter w , which in our case is close to 1. The absorption coefficient α of the applied laser wavelength is higher for amorphous silicon than for polycrystalline silicon, and the thermal conductivity of the amorphous material is almost two orders of magnitude lower than for crystalline silicon. Consequently, according to Eq. (3), the temperature during illumination is expected to be higher for the amorphous material. This means that the temperature of the sample is expected to decrease during the amorphous to crystalline transformation. The temperature change is somewhat less significant if we consider that the thermal conductivity of substrate is also important in determining the heat conduction (16). The value for κ in Eq. (3) would then have a value between that for glass (which remains nearly constant) and that of the thin Si film. Therefore, only after the crystallization process comes to saturation, is the temperature stable, and the peak position reflects the crystal size.

According to above discussion, the increase in the TO peak frequency with time is a consequence of two processes - lowering of the temperature and an increase in crystallized grain size. The instability in the first 20-30 min (see also Fig. 1a) corresponds to the nucleation phase. Further illumination causes the growth of grains up to the saturation value (see also Fig. 1b), which depends upon the irradiation power density (temperature) and the initial hydrogen concentration (Table I). The final grain size, L , in Table I is estimated by the semi empirical relation obtained upon data published in ref. (17), (18):

$$L(\text{\AA}) = 225/(\omega - \omega_0)^{0.76} \quad (4)$$

where L is in \AA , ω the temperature corrected TO peak position and $\omega_0 = 520 \text{ cm}^{-1}$, the value for room-temperature TO peak position of monocrystalline silicon. The temperature values indicated were deduced from the Raman spectra and are expected to be low by about 100K. As is displayed in Table I, higher irradiation power and higher initial hydrogen concentration each lead to smaller crystals. This result, which is similar to results presented in ref. (19) and (20), indicates that in this temperature range, an increase in temperature leads to a higher nucleation rate rather than an increased growth rate, as discussed recently in ref. (21).

TABLE I The illumination power density, average temperature of illuminated volume and average grain size, L , for two samples with different hydrogen concentration.

Power density (kW/cm ²)	Temperature (K) From Raman	L (Å) for sample with 11 at% H	L (Å) for sample with 3 at % H:
150	626	60 ± 10	
170	640	50 ± 10	
190	654	40 ± 8	
230	720	27 ± 6	55± 10
270	900	29 ± 6	45 ± 9

The full width at half maximum of the TO phonon peak versus illumination time for two illumination power densities is plotted in Fig. 5. The FWHM in our case is a consequence of the grain size and the grain size distribution. As is evident in Fig. 5, during the illumination the width decreases only slightly.

CONCLUSION

Thin a-Si:H films, with thickness of ~1 μm and with different hydrogen concentrations, prepared by hot wire deposition were crystallized by 514.5 nm cw Ar ion laser radiation. The power density was varied between 150 and 270 kW/cm⁻¹. The crystallization process, which was analysed using the Johnson-Mehl phenomenological equations, showed an apparent crystallization energy of ~ 0.5 eV and low dimensional crystal growth, resulting in nano crystals with dimensions between 3 and 6 nm. Higher irradiation power and higher initial hydrogen concentration both lead to films with decreased crystalline size.

ACKNOWLEDGMENT

The authors wish to thank A. Soldi for useful suggestions and B. von Roedern for the amorphous silicon samples produced in NREL Golden, Colorado. This work was supported by the NREL subcontract No AAK-9-18675-03. RJN acknowledges the support of the NSF through grant DMR-0102652.

LITERATURE

1. J.H.Werner, R. Bergmann, and R. Brendel, Festkoerperprobleme/Advances in Solid State Physics, Vol. **34**, Ed. R.Helbig, Vieweg, Braunschweig 1994 (p. 115).
2. A.V.Shah, R. Platz, and H. Keppner, Solar Energy Mater, Solar Cells **38** (1995).
3. A. Catalano, Solar Energy Mater. Solar Cells **41/42**, 205 (1996)
4. S.R. Wenham and M.A. Green, Progr. Photovolt., **4**, 3 (1996)
5. E.I. Givargizov, Oriented Crystallization on Amorphous Substrates, Plenum Press, New

- York,,1991.
6. G. Andrae, J.Bergmann, F.Falk, E.Ose, H.Stafast, Phys. Stat. Sol. (a) **166**, 629 (1998)
 - 7.R.B.Bergmann, J.Koehler, R.Dassow, C.Zaczek and J.H.Werner Phys. Stat. Sol. (a) **166**, 578 (1998)
 8. R. Carius, A. Wohllebe, L. Houben, H.Wagner, Phys. Stat. Sol. (a) **166**, 635 (1998)
 9. T.R.Hart, R.L. Aggarwal and B.Lax, Phys. Rev., **1**, 638 (1970).
 10. D.Gracin, M.Jaksic, C.Young, V.Borjanovic and B.Pracek, Appl. Surf. Sci. **144-145**, 188 (1999)
 - 11.S.Inoue, K.Yoshii, M.Umeno, H.Kawabe, Thin Solid Films **151**, 403 (1987) 403
 12. T.R.Hart, R.L.Aggarwal and Benjamin Lax, Phys.Rev.B **1**, 638 (1979)
 13. S.Veprek, F.A.Sarrot and Z.Iqbal, Phys.Rev. B **36** , 3344 (1987)
 14. I.De Wolf, J.Vanhellmont, A.Romano-Rodrigues, N.Nortstroem and H.Maes, J.Appl.Phys. **71**, 898 (1992)
 15. M.Lax, J.Appl.Phys. **48**, 3919 (1977)
 - 16.. M.Ivanda, K.Furic, O.Gamulin, M.Persin and D.Gracin, J.Appl.Phys. **70**, 4637(1991)
 17. Z. Iqbal and S. Veprek, J. Phys. C **15**, 377 (1982)
 18. I. H. Campbell, P.M. Fauchet, Solid State Commun., **58**, 739 (1986)
 19. Militiadis K. Hatalis and David W. Greve, J.Appl.Phys. **63**, 2260 (1988)
 20. R.B. Iverson and R.Reif, J.Appl.Phys.**62**, 1675 (1987)
 21. Z.Ogorelec and A.Tonejc, Materials Letters **42**, 81 (2000)